Strong pinning and elastic to plastic vortex crossover in Na-doped $CaFe_2As_2$ single crystals

N. Haberkorn,[1,*] M. Miura,[1] B. Maiorov,[1] G. F. Chen,[2] W. Yu,[2] and L. Civale[1]
[1]*MPA-STC, Los Alamos National Laboratory, Los Alamos, New Mexico 87545, USA*
[2]*Department of Physics, Renmin University of China, Beijing 100872, China*
(Received 24 June 2011; published 23 September 2011)

We study the vortex dynamics of $Na_xCa_{1-x}Fe_2As_2$ single crystals with $x = 0.5$ (underdoped) and $x = 0.75$ (optimally doped), having $T_c \approx 19.4$ and 33.4 K, respectively, by performing magnetization measurements of the critical current density J_c and flux creep rate S. We find that the J_c versus temperature, T, dependence is consistent with δT_c pinning, indicating strong pinning associated with randomly distributed defects larger than the coherence length ξ. The temperature dependence of S shows a crossover between glassy (elastic) and plastic creep regimes. The boundary $T_{cr}(H)$ between both creep regimes coincides with the upper limit of the regime of strong pinning by nanoparticles. The glassy exponent μ in the optimally doped crystal is consistent with the thermal collective creep theory previously applied to cuprate superconductors, but in the underdoped sample the plateau in $S(T)$ indicates that $\mu \approx 3$–3.3, a value larger than the existing theoretical predictions. We discuss the quantum creep contributions in both samples.

DOI: 10.1103/PhysRevB.84.094522 PACS number(s): 74.25.Wx, 74.25.Sv, 74.70.Xa

I. INTRODUCTION

One of the most fascinating dynamics phenomena of complex systems is the thermally activated flux creep in high-temperature superconductors (HTS). The discovery of superconductivity in layered iron arsenides opens the possibility to extend the study of vortex dynamics to superconductor materials with intermediate properties between conventional low-temperature superconductors and cuprates. Iron arsenide superconductors of the type AFe_2As_2 (122 system), where A is an alkaline-earth element, show intermediate superconducting transition temperatures T_c between conventional and cuprate superconductors, low anisotropy ($\gamma \approx 2$), as well as high upper critical fields H_{c2} due to the concomitant small coherence lengths ξ.[1] High flux creep rates and a transition from collective to plastic creep have been reported in Co-doped $BaFe_2As_2$; the transition between the two regimes was associated with a second peak in the magnetization (SPM)[2,3] similar to what was previously found in $YBa_2Cu_3O_{7-x}$ single crystals.[4] However, we showed that in Na-doped $CaFe_2As_2$ single crystals the SPM does not appear,[5] indicating that the origin of the pinning is different from that found in Co-doped $BaFe_2As_2$. We also found that over large regions of the temperature-field phase diagram the pinning in our crystals is dominated by a sparse random distribution of nanoparticles.[5] On the other hand, Nakajima *et al.*[6] showed that, as in $YBa_2Cu_3O_{7-x}$ single crystals,[7] it is possible to improve the critical currents J_c in Co-doped $BaFe_2As_2$ by the introduction of columnar defects.

Although in principle the ideas of glassy vortex dynamics and the collective creep theory are general and not restricted to a particular type of superconductor, in reality they were originally developed for HTS cuprates[8] where, due to the short ξ and large γ, the pinning energy U_0 is very small and the creep rate is high. In contrast, low-T_c superconductors (LTS) typically have much smaller creep rates and the differences between the classical Anderson-Kim and the glassy descriptions are hard to observe.[8,9] Thus, the similarity in the vortex dynamics of pnictides and cuprates[2,4] makes the iron-arsenide-based materials ideal to deepen and generalize our understanding of vortex matter.

In this work we analyze the vortex pinning and dynamics by magnetization M as a function of magnetic field $\mathbf{H}$, temperature T, and time t (flux creep measurements) on Na-doped $Na_xCa_{1-x}Fe_2As_2$ single crystals with $x = 0.5$ (underdoped) and $x = 0.75$ (optimally doped), having $T_c \approx 19.4$ and 33.4 K, respectively. The results obtained in both single crystals show that the temperature dependence of the flux creep rate S shows a crossover between collective elastic and plastic creep regimes. In both cases the elastic creep is consistent with strong pinning given by a small density of nanoparticles, but the glassy exponent μ for the elastic collective creep is very different in the two samples. For the optimally doped crystal $\mu \approx 0.7$–1, a value frequently observed in $YBa_2Cu_3O_7$ and consistent with expectations for collective creep regimes, while for the underdoped crystal $\mu \approx 3$–3.3, which is above the highest μ predicted by collective creep models.

The activation energy as a function of current density J in a glassy vortex phase is

$$U(J) = \left(\frac{U_0}{\mu}\right)\left[\left(\frac{J_c}{J}\right)^{\mu} - 1\right], \tag{1}$$

where $\mu > 0$ is the glassy exponent and U_0 is the characteristic pinning energy. The time decay of J is given by the interpolation between the classical Anderson-Kim model and the nonlinear logarithmic time and the current density:

$$J = J_c\left[1 + \frac{\mu T}{U_0}\ln(t/t_0)\right]^{-1/\mu}, \tag{2}$$

where t_0 is a characteristic time and T is the temperature. The normalized relaxation rate is

$$S = -\frac{d(\ln J)}{d(\ln t)} = \frac{T}{U_0 + \mu T \ln(t/t_0)} = \frac{T}{U_0}\left(\frac{J}{J_c}\right)^{\mu}. \tag{3}$$

The condition $\mu > 0$ implies a diverging activation energy as $J \to 0$ in Eq. (1), which is a consequence of the elasticity of the vortex matter, so this is also called elastic creep. The glassy exponent μ is regime dependent. For instance, for random

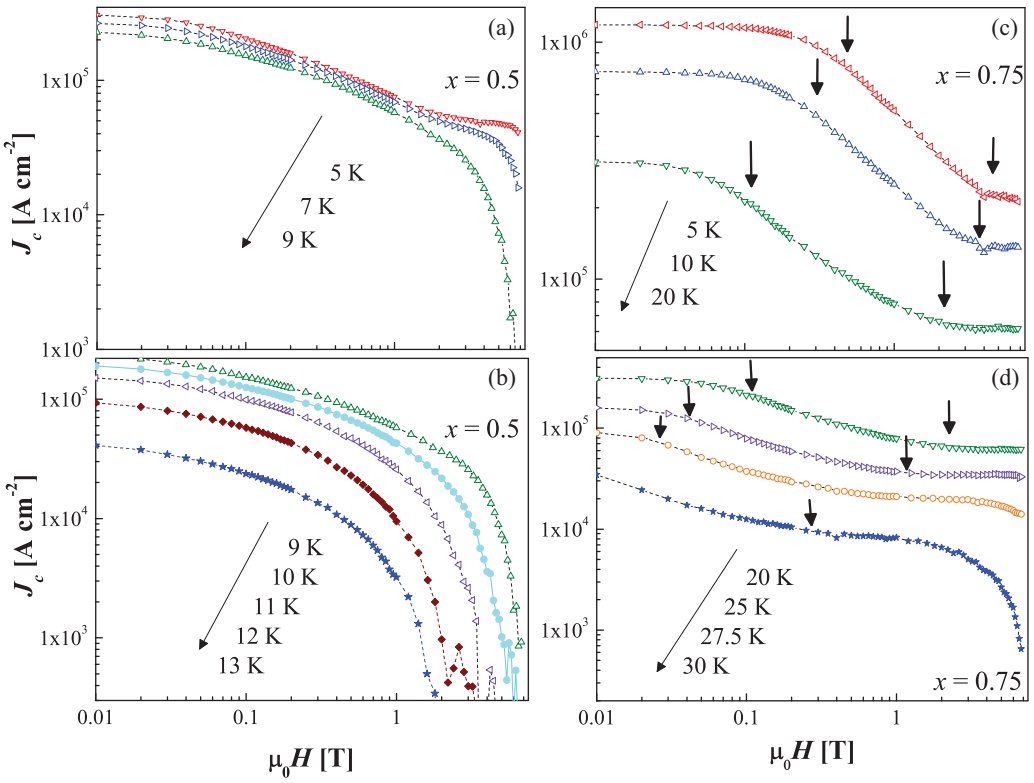

FIG. 1. (Color online) Magnetic field (H) dependence of the critical current density (J_c) at different temperatures. (a), (b) $x = 0.5$; (c), (d) $x = 0.75$. Black arrows indicate the start and the end of the power-law regime $J_c \propto H^{-\alpha}$.

point disorder the collective creep model predicts $\mu = 1/7$ for single vortex creep, 3/2 or 5/2 for small bundles, and 7/9 for large bundles, while different μ values are expected for correlated disorder in various single-vortex and collective regimes. Experimentally, a large number of μ values have been reported.[2]

If we define the vortex creep energy $U^* = U_0 + \mu T \ln(t/t_0)$ we obtain

$$U^* = \frac{T}{S} = U_0^e \left(\frac{J_c}{J}\right)^{\mu}. \quad (4)$$

The same expressions can be used to describe a plastic creep (nondiverging U for $J \to 0$) by taking $\mu < 0$. In particular, $\mu = -1$ corresponds to the classical Anderson-Kim model. The plastic exponent is commonly called p; thus in the plastic regime we have

$$U^* = \frac{T}{S} = U_0^p \left(\frac{J_c}{J}\right)^{p}. \quad (5)$$

By the analysis of U^* versus $\frac{1}{J}$ it is possible to estimate the crossover between different creep regimes and the pinning energy.[10] It is also well known that a logarithmic current dependence, $U_{(J)} = U_0 \ln(\frac{J_c}{J})$,[11] which formally corresponds to $\mu \to 0$, is often a very good description of experimental data, and in this case $U^* = U_0$.

II. EXPERIMENTAL DETAILS

Single crystals of $Na_xCa_{1-x}Fe_2As_2$ with $x = 0.5$ and $x = 0.75$ have been grown by a self-flux technique. Both samples are superconducting with T_c of 19.4 and 33.4 K, respectively. These values agree with those previously reported for similar chemical composition.[12,13] The details of the sample preparation and characterization were presented elsewhere.[5] In all cases a 100% superconducting volume fraction was observed, as was previously discussed.[5]

The irreversible magnetization $M(H,T)$ was measured in a commercial superconducting quantum interference device magnetometer, and used to calculate $J_c(H,T)$ according to the Bean critical-state model.[14] The time relaxation of the irreversible magnetization $M(t)$, which is proportional to $J_c(t)$, was measured (typically for 1 h) to determine the flux creep rates. For each T and H the initial critical state was generated by reducing the field to the measuring value H from $H + \Delta H$ with $\Delta H \approx 4H^*$, where H^* is the first magnetic field for full flux penetration. [9]

III. RESULTS

Figure 1 shows $J_c(H)$ for $\mathbf{H} \| c$ at several T for both single crystals (SCs) in log-log scale. These data were previously shown and discussed in Ref. 5. In contrast to previous reports on 122 single crystals with different composition,[2,3] we do not observe a second peak in the critical current density. However, $x = 0.75$ shows a region where $J_c(H) \approx$ constant, as was previously discussed.[5] In order to understand the vortex dynamics in these samples we performed magnetic relaxation measurements. For a clearer presentation, the measurements in each one of the SCs will be shown separately.

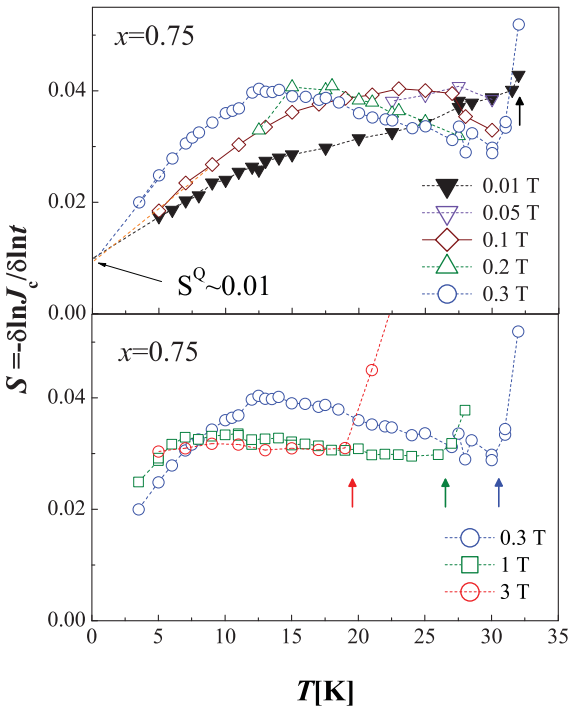

FIG. 2. (Color online) Temperature dependence of the creep rates (S) at different applied magnetic fields (H) in $x = 0.75$. The arrows indicate $T_{cr}(H)$.

A. Optimally doped sample ($Na_{0.25}Ca_{0.75}Fe_2As_2$)

Figure 2 shows $S(T)$ in $x = 0.75$, obtained from isothermal magnetization relaxation using Eq. (3). The main features in $S(T)$ are (i) The high vortex creep rates ($0.02 < S < 0.04$) are in the same range as those previously reported in YBCO.[8,9] (ii) $S(T)$ at low H shows a peak, with the maximum at a temperature that decreases when H is increased. The S value at the maximum is always the same (~0.04). (iii) This peak disappears above $\mu_0 H \approx 1$ T, and $S(T)$ shows a plateau in agreement with collective vortex theory (glassy relaxation).[8,9] Also, for $\mu_0 H < 1$ T the $S(T)$ values above the peak tend to be ~0.03, which is the value at the plateau. (iv) For all fields $S(T)$ shows a sudden increase at a field-dependent temperature $T_{cr}(H)$, indicated by arrows in Fig. 2. At low H this crossover to fast creep appears at $T \approx 30$ K ($\sim 0.95 T_c$).

Figure 3 shows the U^* versus $\frac{1}{J}$ dependence for $x = 0.75$ at $\mu_0 H = 1$ T, which is the H value where the peak in $S(T)$ disappears. Using Eqs. (4) and (5), we obtain $\mu \approx 0.7$ and $p \approx -0.5$ (red dashed lines) as is expected for collective creep by large bundles and plastic creep, respectively.[8,15] On the other hand, if we consider that in the plateau $S = [\mu \ln(t/t_0)]^{-1} \approx 0.03$, where $\ln(t/t_0) \approx 30$, we get $\mu \approx 1$. The normalized vortex creep energy at the crossover between both regimes is ~900 K.

The pinning in type II superconductors may originate in disorder in T_c (δT_c) and/or from the spatial variation in the free path l near a lattice defect (δl).[8] In the single vortex regime J_c can be expressed as a function of the temperature as $J_c \propto [1 - (\frac{T}{T_c})^2]^n$, where the exponent n indicates the type of pinning, being 7/6 and 5/2 for δT_c and δl pinning, respectively.[16] Figure 4 shows J_c versus $1 - (\frac{T}{T_c})^2$ at $\mu_0 H = 0$; 0.3 and 1 T for $x = 0.75$. The data fit with $n = 1.4$, which

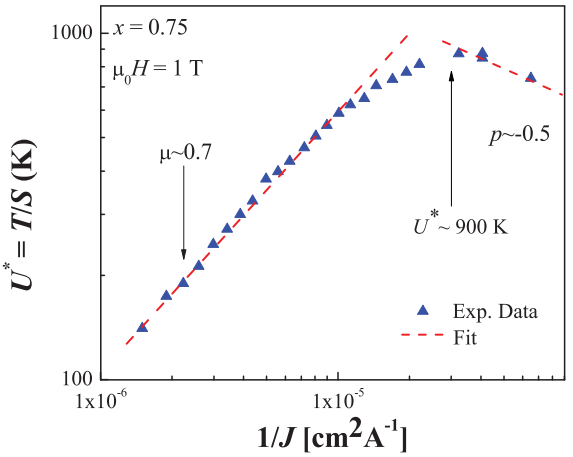

FIG. 3. (Color online) U^* versus $1/J$ obtained using the relaxation creep data for $\mu_0 H = 1$ T shown in Fig. 2 ($x = 0.75$). The creep crossover appears at ~27 K. The red dashed straight lines are fits to Eqs. (4) and (5). In the elastic collective creep $\mu \sim 0.7$ is obtained, whereas in the plastic regime $p \approx -0.5$ is obtained.

is close to the expectation for δT_c pinning.[17] The δT_c pinning remains dominant up to temperatures close to T_c, similar to the case of YBCO films with strong pinning by nanoparticles.[18]

B. Underdoped sample ($Na_{0.5}Ca_{0.5}Fe_2As_2$)

Figure 5(a) shows the $S(T)$ dependence at $\mu_0 H = 0.3$ T for $x = 0.5$. The results show a plateau between 4 and 10 K ($S \sim 0.01$); above $T \approx 10$ K the S values start to increase. Figure 5(b) shows $S(H)$ at several T; it is clear that the plateau with $S \approx 0.01$ remains independent of H. However, the crossover to fast creep occurs at progressively lower T when H is increased. Figure 6 shows the U^* versus $\frac{1}{J}$ dependence [see Eqs. (4) and (5)] for the data presented in Fig. 5(a). The results indicate a crossover from collective to plastic creep; the value of $\mu \approx 3$ indicates a glassy behavior with a value higher than the predictions of the collective creep theory, whereas $p \approx -0.4$ is the value expected for plastic creep of dislocation bundles.[15] From the plateau $S = [\mu \ln(t/t_0)]^{-1} \approx 0.01$, where

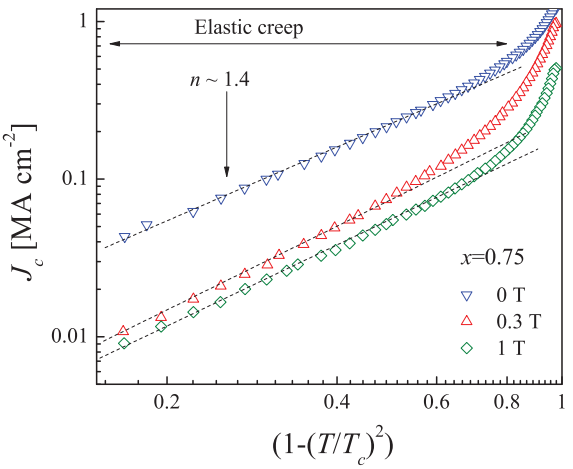

FIG. 4. (Color online) Log-log plot of J_c versus $1 - (\frac{T}{T_c})^2$ at different H values in $x = 0.75$. Straight lines correspond to the best fits to obtain the n value.

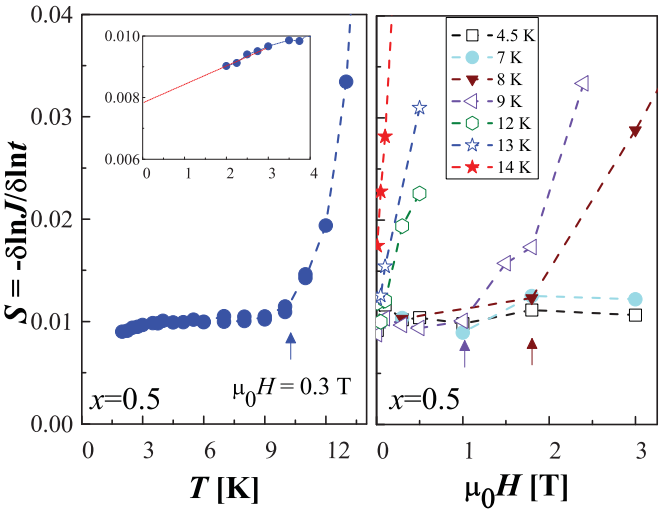

FIG. 5. (Color online) Temperature dependence of the creep rate (S) at $\mu_0 H = 0.3$ T in $x = 0.5$ (left). $S(H)$ dependence at different temperatures in $x = 0.5$ (right). The arrows indicate $T_{cr}(H)$. Inset: expanded view of $S(T)$ of the low temperature range.

$\ln(t/t_0) \approx 30$, we get a similar estimate, $\mu \approx 3.3$. Finally, the $S(T)$ extrapolation to $T = 0$ K, which corresponds to quantum creep S^Q, gives $S(0) \approx 0.075$, indicating a nonnegligible quantum contribution at low temperatures (see inset Fig. 5).

Figure 7 shows the J_c versus $1-(\frac{T}{T_c})^2$ dependence at different H. The linear fits at low T (in the elastic regime) correspond to $n = 1.2$, as expected for δT_c pinning due to the presence of small precipitates.[16–18] As T increases we observe a crossover to a larger slope n in Fig. 7 [faster decay of $J_c(T)$]. The crossover temperature is ~11 K ($T \approx 0.6T_c$) at self-field and decreases as H increases. It is important to remark that also at temperatures above ~11 K the power law $J_c \propto H^{-\alpha}$ disappears [see Figs. 2(a) and 2(b)]. This suggests that the nanoparticles or strong pinning centers that are effective at low temperatures become less effective above ~11 K. This scenario is consistent with our previous analysis of the pinning force, where a change in the pinning mechanism was observed around 10 K.[5]

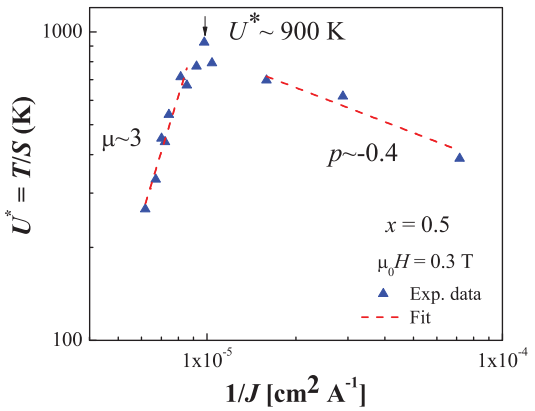

FIG. 6. (Color online) U^* versus $1/J$ from the relaxation data for $\mu_0 H = 0.3$ T shown in Fig. 5. The creep crossover appears at 10 K. The red dashed straight lines are fits to Eqs. (4) and (5). In the elastic collective creep $\mu \approx 3$ is obtained, whereas in the plastic regime $p \approx 0.4$ is obtained.

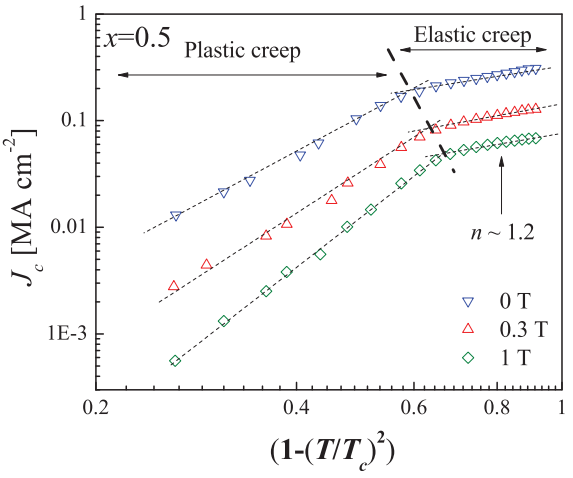

FIG. 7. (Color online) Log-log plot of J_c versus $1-(\frac{T}{T_c})^2$ at different H in $x = 0.5$. Straight lines correspond to the best fit in both regimes.

IV. DISCUSSION

Our study shows that both single crystals present a crossover between collective elastic and plastic (fast) creep at a field-dependent temperature $T_{cr}(H)$ as shown in the phase diagrams in Fig. 8. The T_{cr}/T_c ratio is very different in the two materials; for instance at self-field it is $\sim 0.6T_c$ and $\sim 0.95T_c$ for $x = 0.5$ and $x = 0.75$, respectively. In both crystals there is a clear coincidence between $T_{cr}(H)$ and the location of the upper end of the power-law regime $J_c \propto H^{-\alpha}$ with $\alpha \approx 0.55$, indicated by arrows in Fig. 1 and also included in Fig. 8. We had

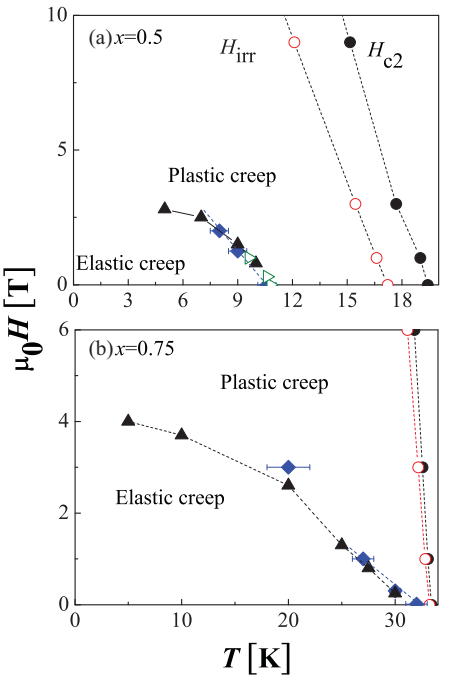

FIG. 8. (Color online) The vortex phase diagrams for both single crystals: (a) $x = 0.5$; (b) $x = 0.75$. Blue diamond: creep crossover. Black triangle: end of the power-law regime in $J_c(H)$. In figure (a) (open green triangle) the temperature crossover obtained from Fig. 7 is also included. H_{c2} and H_{irr} were taken from Ref. 5.

previously shown that the $J_c \propto H^{-\alpha}$ regime is associated with pinning by randomly distributed nanoparticles. Also, as shown in Figs. 4 and 7, in both crystals the $J_c(T)$ dependence below the $T_{cr}(H)$ crossover is characterized by n values consistent with δT_c pinning, a mechanism usually associated with the presence of defects larger than the coherence length ξ.[16,17] In the underdoped crystal (see Fig. 7) we can also track the H dependence of the crossover from $n \sim 1.2$ at low T to a faster J_c decay at higher T. That boundary is also included in the phase diagram [Fig. 8(a)] and again coincides remarkably well with $T_{cr}(H)$. In the optimally doped crystal this crossover in $J_c(T)$ occurs too close to T_c to be satisfactorily determined. As we have previously shown that neither of the two crystals has significant pinning arising from correlated disorder,[5] the coincidence of the various features in the phase diagrams of Figs. 8(a) and 8(b) demonstrate that the elastic creep regime below $T_{cr}(H)$ corresponds to strong pinning associated with the presence of a random distribution of nanoparticles.[19,20] The identification of the nanoparticles in our crystals will require careful microstructural studies.

We now discuss the nature of the crossover at $T_{cr}(H)$. If vortex pinning below $T_{cr}(H)$ arises from nanoparticles with radius r_d of a few nanometers, then the vortex dynamics can be analyzed in analogy with columnar defects.[8,19] A crossover from a strong pinning regime at low T to weaker pinning at high T is expected when $\sqrt{2}\xi(T) = r_d$, where $\xi(T) = \xi(0)(1-T/T_c)^{1/2}$ is the temperature-dependent coherence length, at a temperature T_{cr} defined by $\frac{T_{cr}}{T_c} = 1 - \frac{2\xi^2(0)}{r_d^2}$.[8] If we assume $\xi(0) = 3.68$ nm for $x = 0.5$ and $\xi(0) = 2.1$ nm for $x = 0.75$,[5] in the case of $x = 0.5$ using $T_{cr} = 11$ K we get $r_d \approx 5$ nm. In the case of $x = 0.75$, on the other hand, nanoparticles of the same size would produce strong pinning up to temperatures very close to T_c, similar to the situation frequently observed in YBCO films.[18] Thus, the different T_{cr}/T_c ratios in our two crystals is a manifestation of the general rule that defects of size smaller than the vortex core are weak pinning centers. Again by analogy with the case for columnar defects, the field dependence of $T_{cr}(H)$ can be associated with an accommodation field. Following these considerations, the creep rate will be fast above $T_{cr}(H)$, when only a fraction of vortices are strongly pinned, whereas the rest are only retained by the shear force within the lattice.[8] This also initiates a change in the vortex dynamics, with an increase in the creep rate and a crossover from elastic to plastic creep.

In the elastic creep regime, both crystals show a plateau in $S(T)$ over a wide T-H range. This is a clear fingerprint of a glassy relaxation regime defined by a single μ value. To our knowledge, there are no theoretical predictions for the glassy exponents expected for strong pinning by randomly distributed nanoparticles. In $x = 0.75$ the glassy exponent $\mu \approx 0.7$–1 is within the range typically observed in YBCO, and consistent with the expectations for collective creep of large bundles in the case of random point disorder. The plateau starts at $T \approx 5$ K, indicating that the pinning energy $U_0 \approx \mu T \ln(t/t_0) \approx 100-150$ K.

As we showed previously, in $x = 0.75$ the $S(T)$ dependence at low fields ($\mu_0 H \leqslant 0.3$ T) shows a peak (see Fig. 2). In cuprate superconductors like YBCO single crystals and films, a peak in $S(T)$ associated with double kink and superkink

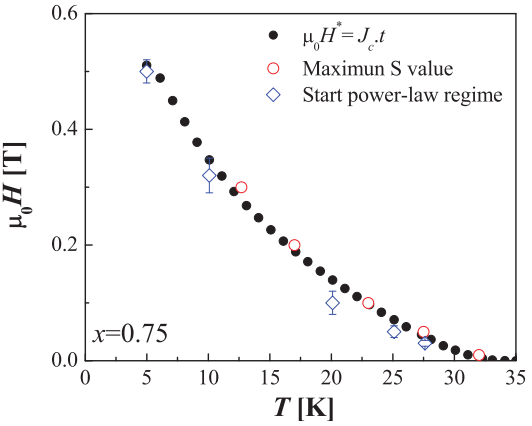

FIG. 9. (Color online) Temperature dependence of the $S(T)$ maximum value (see Fig. 2), and the self-field estimated as $H^* = J_c^{H=0} \times$ thickness and as the H where the J_c (H) power-law regime starts (see Fig. 1), in crystal $x = 0.75$.

depinning excitations is observed in the presence of correlated disorder (columnar defects).[21] In $x = 0.75$ the anisotropic scaling of the irreversibility line and the $J_c(H)$ dependence for **H** tilted with respect to the c axis indicates the absence (or negligible influence) of correlated disorder.[5] Also, the peak in $x = 0.75$ shows clear differences from the peak produced by columnar defects in YBCO. Whereas in the $S(T)$ peak associated with columnar defects the value of S at the maximum decreases when H is increased (due to a filling effect) and the temperature of the maximum is weakly affected, in the $x = 0.75$ the S value at the maximum is always the same ($\sim$0.04) and the T where the maximum occurs decreases strongly when H is increased. Considering these differences, the interpretation for this peak should be different. According to Taen *et al.*[22] a suppression of the S values at low temperatures occurs when the applied H is smaller than the maximum self-field in the sample, this suppression being a consequence of the "Meissner hole" that appears close to the edges of the sample.[23] In order to analyze this possibility, in Fig. 9 we compared the T dependence of the self-field, estimated both as $H^* = J_c^{H=0} \times$ thickness, and from the start field of the power-law regime [see arrows in Figs. 1(c) and 1(d)], with the temperature where the maximum in S occurs for each applied H. Clearly we get a very good agreement, indicating that the vortex dynamics at $\mu_0 H < \mu_0 H^*$ are strongly affected by the magnetic field inhomogeneity associated with self-field effects.

In contrast to $x = 0.75$, in the case of $x = 0.5$ the obtained $\mu \approx 3$–3.3 is larger than the expectations of the collective creep scenario as well as the predictions for correlated disorder.[8] If only thermal creep were present, the fact that the plateau in $S(T)$ extends to T as low as $\sim$3.5 K would indicate a pinning energy $U_0 \approx \mu T \ln(t/t_0) \approx 300$ K. However, this estimate should be taken with caution due to the significant quantum creep contribution, as we discuss later. We find that $x = 0.5$ does not show a peak in the $S(T)$ dependence. The probable reason is that the self-field is smaller than in $x = 0.75$, being $\mu_0 H^* \approx 0.09$ T at 5 K and $\mu_0 H^* \approx 0.05$ T at 10 K (see Fig. 9).

Finally, we are going to discuss the presence of quantum creep in both samples [see Figs. 2(a) and (5)].[8] At low temperatures where the quantum creep dominates, S is given by

$$S^Q \cong \frac{e^2}{\hbar}\frac{\rho_n}{\xi}\left(\frac{J_c}{J_0}\right)^{1/2},$$

where ρ_n is the resistance in the normal state, J_0 is the depairing critical current density, and $\frac{\hbar}{e^2} = 4108\ \Omega$. Using ρ_n of 140 $\mu\Omega$ cm and 110 $\mu\Omega$ cm, obtained from $\rho(T)$ measurements in our crystals,[5] we estimate $S = 0.006$ and $S = 0.008$, for $x = 0.5$ and $x = 0.75$, respectively, in good agreement with the experimental results. In $x = 0.5$, the plateau in S that is H independent at low temperatures ($S \sim 0.01$) is very close to the extrapolated quantum creep value ($S \sim 0.075$), and suggests that the creep below 10 K could have an important quantum contribution. The quantum tunneling probability of a vortex segment without environmental interaction $\propto \exp^{-U/\hbar\omega_0}$ is bigger than the chance of thermal activation $\propto \exp^{-U/k_BT}$, whereas $\hbar\omega_0 \geqslant k_BT$, where ω_0 is the depinning frequency.[24] In particular, for YBCO the quantum creep contributes below 10 K.[24]

By combining these results we obtain a remarkably consistent characterization of the vortex pinning and dynamics in our crystals, as shown in the phase diagrams in Fig. 8. Both samples show qualitatively similar behavior, with elastic collective creep at low T and H and a crossover to plastic (fast) creep regime above a $T_{cr}(H)$ boundary. This boundary coincides with the upper end of the power-law regime $J_c \propto H^{-\alpha}$ originating in the strong pinning by sparse random nanoparticles. As within the power-law regime the vortices are interacting, thus the creep mechanism must be associated with depinning of vortex bundles. However, the glassy exponent μ is quite dissimilar in the two single crystals, indicating that even though the pinning landscape is similar in both crystals the creep regimes are different. An important difference between both samples is the size of the vortex core. As discussed previously, the low $T_{cr}(H = 0) \approx 0.6T_c$ in $x = 0.5$ is consistent with a regime crossover at $\sqrt{2}\xi(T) = r_d$, not observed in $x = 0.75$ due to its smaller ξ_0. Nakajima *et al.*[6] showed that in Co-doped $BaFe_2As_2$ single crystals the introduction of defects by heavy ion irradiation improves J_c and also increases the magnetic field crossover between creep regimes at 15 K. This is consistent with an increase in T_{cr} due to larger defects.

Although the smaller creep rate in $x = 0.5$ as compared to $x = 0.75$ can be expected by the simple consideration that it has lower T_c and smaller Ginzburg number Gi, the nontrivial observation is that it exhibits a glassy relaxation with a μ larger than predicted and observed in cuprates. The largest μ values predicted by the models are associated with small bundles; however, from the J_c/J_0 ratios in $x = 0.5$ large rather than small bundles should be expected, with μ values around 1 or smaller. More generally, larger μ indicates more interactive vortices. Our results point to the need to explore more examples of vortex matter in systems where the influence of thermal fluctuations is intermediate between the case of conventional and HTS. Finally, the crossover from elastic to plastic creep has been observed in several Fe-As 122 compounds as well as in cuprates, and associated with different pinning regime crossovers. Our results highlight the importance of the ratio of defect and vortex core sizes, but a general picture must clearly include other variables such as defect density and shape.

V. CONCLUSION

In summary, we have studied the vortex dynamics in Na-doped $CaFe_2As_2$ single crystals by magnetization measurements of the critical current density and its time relaxation. We observed a crossover from collective elastic to plastic creep in both crystals. In the underdoped crystal the crossover temperature is $T_{cr} \approx 0.6T_c$, whereas in the optimally doped crystal the crossover is close to T_c ($\sim 0.95T_c$). The T_{cr} could be associated with the ratio of defect size to $\xi(T)$. The glassy exponent for the elastic creep is very different in each sample, $\mu \approx 0.7$ and $\mu \approx 3$ for optimally doped and underdoped, respectively. While the first one is consistent with theoretical models for the collective creep of large bundles, the second one is larger than those predictions and points to the presence of an alternative type of depinning excitations, where quantum creep may play a significant role.

ACKNOWLEDGMENTS

Research at LANL was supported by the US Department of Energy, Office of Basic Energy Sciences, Division of Materials Sciences and Engineering (magnetometry, data analysis, manuscript preparation). Work by G.F.C. and W.Y. (fabrication of samples) was supported by the NSFC under Grant Nos. 10974254 and 11074304, and by the National Basic Research Program of China under Grant Nos. 2010CB923000 and 2011CBA00100. N.H. is member of CONICET (Argentina).

*nhaberkorn@lanl.gov

[1] J. Paglione and R. L. Greene, Nat. Phys. **6**, 645 (2010).
[2] R. Prozorov, N. Ni, M. A. Tanatar, V. G. Kogan, R. T. Gordon, C. Martin, E. C. Blomberg, P. Prommapan, J. Q. Yan, S. L. Bud'ko, and P. C. Canfield, Phys. Rev. B **78**, 224506 (2008).
[3] B. Shen, P. Cheng, Z. Wang, L. Fang, C. Ren, L Shan, and H.-H. Wen, Phys. Rev. B **81**, 014503 (2010).
[4] Y. Abulafia, A. Shaulov, Y. Wolfus, R. Prozorov, L. Burlachkov, Y. Yeshurun, D. Majer, E. Zeldov, H. Wühl, V. B. Geshkenbein, and V. M. Vinokur, Phys. Rev. Lett. **77**, 1596 (1996).
[5] N. Haberkorn, B. Maiorov, M. Jaime, I. Usov, M. Miura, G. F. Chen, W. Yu, and L. Civale, Phys. Rev. B **84**, 064533 (2011).
[6] Y. Nakajima, Y. Tsuchiya, T. Taen, T. Tamegai, S. Okayasu, and M. Sasase, Phys. Rev. B **80**, 12510 (2009).
[7] J. R. Thompson, L. Krusin-Elbaum, L. Civale, G. Blatter, and C. Feild, Phys. Rev. Let. **78**, 3181 (1997).
[8] G. Blatter *et al.*, Rev. Mod. Phys. **66**, 1125 (1994).
[9] Y. Yeshurun, A. P. Malozemoff, and A. Shaulov, Rev. Mod. Phys. **68**, 911 (1996).
[10] L. Miu and D Miu, Supercond. Sci. Technol. **23**, 025033 (2010).
[11] E. Zeldov, N. M. Amer, G. Koren, A. Gupta, M. W. McElfresh, and R. J. Gambino, Appl. Phys. Lett. **56**, 680 (1990).

[12]K. Zhao, Q. Q. liu, X. C. Wang, Z. Deng, Y. X. lv, J. L. Zhu, F. Y. Li, and C. Q. Jin, J. Phys.: Condens. Matter **22**, 222203 (2010).
[13]G. Wu, H. Chen, T. Wu, X. L. Xie, Y. J. Yan, R. H. Liu, X. F. Wang, J. J. Ying, and X. H. Chen, J. Phys.: Condens. Matter **20**, 422201 (2008).
[14]C. P. Bean, Phys. Rev. Lett. **8**, 250 (1962); Rev. Mod. Phys. **36**, 31 (1964).
[15]J. Kierfeld, H. Nordborg, and V. M. Vinokur, Phys. Rev. Lett. **85**, 4948 (2000).
[16]A. O. Ijaduola, J. R. Thompson, R. Feenstra, D. K. Christen, A. A. Gapud, and X. Song, Phys. Rev. B **73**, 134502 (2006).
[17]R. Griessen, W. Hai-hu, A. J. J. van Dalen, B. Dam, J. Rector, H. G. Schnack, S. Libbrecht, E. Osquiguil, and Y. Bruynseraede, Phys. Rev. Lett. **72**, 1910 (1994).
[18]M. Miura, B. Maiorov, S. A. Baily, N. Haberkorn, J. O. Willis, K. Marken, T. Izumi, Y. Shiohara, and L. Civale, Phys. Rev. B **83**, 184519 (2011).
[19]C. J. van der Beek, M. Konczykowski, A. Abal'oshev, I. Abal'osheva, P. Gierlowski, S. J. Lewandowski, M. V. Indenbom, and S. Barbanera, Phys. Rev. B **66**, 024523 (2002).
[20]C. J. van der Beek, G. Rizza, M. Konczykowski, P. Fertey, I. Monnet, Thierry Klein, R. Okazaki, M. Ishikado, H. Kito, A. Iyo, H. Eisaki, S. Shamoto, M. E. Tillman, S. L. Bud'ko, P. C. Canfield, T. Shibauchi, and Y. Matsuda, Phys. Rev. B **81**, 174517 (2010).
[21]J. R. Thompson, L. Krusin-Elbaum, L. Civale, G. Blatter, and C. Feild, Phys. Rev. Lett. **78**, 3181 (1997).
[22]T. Taen, Y. Tsuchiya, Y. Nakajima, and T. Tamegai, Phys. C **470**, 1106 (2010).
[23]V. K. Vlasko-Vlasov, U. Welp, G. W. Crabtree, D. Gunter, V. Kabanov, and V. I. Nikitenko, Phys. Rev. B **56**, 5622 (1997).
[24]A. F. Th. Hoekstra, A. M. Testa, G. Doornbos, J. C. Martinez, B. Dam, R. Griessen, B. I. Ivlev, M. Brinkmann, K. Westerholt, W. K. Kwok, and G. W. Crabtree, Phys. Rev. B **59**, 722 (1999).